Comprehensive genomic characterization of programmed cell death-related genes to predict drug resistance and prognosis for patients with multiple myeloma

Yan Li[1], Fuxu Wang[2], Hongbo Zhao[1], Zhenwei Jia[1], Xiaoyan Liu[1], Guirong Cui[1], Tiejun Qin[3], Xiaoyang Kong[1]

[1]Hematology Department, Handan First Hospital, Handan 056001, China
[2]Department of Hematology, Key Laboratory of Hematology of Hebei Province, Second Hospital of Hebei Medical University, Shijiazhuang 050000, China
[3]MDS and MPN Centre, Institute of Haematology and Blood Diseases Hospital, Tianjin 300020, China

Correspondence to: Yan Li; **email:** handanliyan68@sohu.com, https://orcid.org/0009-0002-2976-2167

ABSTRACT

Background: Multiple myeloma (MM) is a cancer that is difficult to be diagnosed and treated. This study aimed to identify programmed cell death (PCD)-related molecular subtypes of MM and to assess their impact on patients' prognosis, immune status, and drug sensitivity.

Methods: We used the ConsensusClusterPlus method to classify molecular subtypes with prognostically relevant PCD genes from the MM patients screened. A prognostic model and a nomogram were established applying one-way COX regression analysis and LASSO Cox regression analysis. MM patients' sensitivity to chemotherapeutic agents was predicted for at-risk populations.

Results: Six molecular subtypes were classified employing PCD-related genes, notably, three of them had a higher tendency for immune escape and two of them were correlated with a worse prognosis of MM. Furthermore, the C3 subtype had activated pathways such as oxidative phosphorylation and DNA repair, while the C2 and C4 subtypes had activated pathways related to apoptosis. The Risk score showed that the nomogram can correctly predict the OS for MM patients, in particular, patients in the high-risk group had low overall survival (OS). Pharmacovigilance analyses revealed that patients in the high-risk and low-risk groups had greater IC_{50} values for the drugs SB505124_1194 and AZD7762_1022, respectively.

Conclusions: A 12-gene Risk score model developed with PCD-related genes can accurately predict the survival for MM patients. Our study provided potential targets and strategies for individualized treatment of MM.

INTRODUCTION

Multiple myeloma (MM) is the second most frequent hematological tumor [1–3]. Around 10% of all hematological malignancies are MM cases, with the majority of patients over 40 years of age and a 5-year survival rate of 53% [4, 5]. Multifocal spread throughout the bone marrow without apparent clinical symptoms is the main characteristic of early-stage MM. In the last ten years, the advent of immunomodulatory medications, proteasome inhibitors, and combination therapy has improved the treatment of MM. For instance, immuno-modulator drugs (IMiDs) are considered as a single-agent maintenance therapy after autologous stem cell transplantation and can be used in combination therapy for all stages of MM [6]. Daratumumab, the first CD38 monoclonal antibody medication authorized for the treatment of MM patients, has shown promising effect on

treating both newly diagnosed MM and relapsed or refractory MM [7]. Nevertheless, MM is still largely incurable and many patients relapse due to immune evasion and therapeutic resistance [8, 9], necessitating the discovery of novel molecular biomarkers to improve patient risk classification and therapy response prediction.

Since the primary objective of cancer treatment is to eradicate tumor cells, inducing cancer cell death has become a crucial strategy [10]. The active process of programmed cell death (PCD) preserves bodily growth and survival [10], while non-PCD is a highly structured process that typically involves the regulation of gene expression and signal transmission [11]. In contrast, PCD is a type of necrosis stimulated by trauma, infection, or ischemia [12]. Although the morphology, biochemistry, and signaling pathways of different forms of cell death vary, they are all actively executed by cells as a part of PCD process, which is essential for maintaining tissue homeostasis and supporting the immune system [13, 14]. Moreover, the development of numerous diseases, including immunological problems, tissue damage, neurodegeneration as well as malignancies such as MM [15], breast cancer [12] and hepatocellular carcinoma [16], are closely linked to PCD. Furthermore, there is a strong correlation between the prognostic evaluation of cancer patients and PCD-related genes. Gu et al. discovered five important PCD genes [17] that affect hepatocellular carcinoma patients by controlling immunological function, inflammatory pathways, and treatment response. Recent evidence suggested that PCD-associated genes contribute to the prognostic prediction, immune profile, and treatment of endometrial cancer of the uterine corpus [18]. Similarly, PCD-associated traits have been identified to evaluate the immune micro-environment landscape, drug sensitivity and prognosis for patients with cutaneous melanoma [19] and acute myeloid leukemia [20]. Based on the above findings, the present work classified molecular subtypes of MM based on prognostically significant PCD-related genes by consensus clustering method, and further compared the differences between the subtypes in terms of pathway characteristics and clinical features. Differential expression analysis and LASSO were employed to determine genes related to PCD phenotype. Finally, we constructed a clinical prognostic model to offer novel understanding for the targeted drug therapy and clinical diagnosis of adjuvant MM.

MATERIALS AND METHODS

Data collection

The Cancer Genome Atlas (TCGA, https://portal.gdc.cancer.gov/) database was accessed to obtain the RNA-seq data, corresponding clinical characteristics, and

follow-up data of 859 MM patients from the MMRF-COMPASS project. A total of 844 MM samples were obtained after data preprocessing. Then, these samples were randomly assigned into training set (592 cases) and validation set (252 cases) at the ratio of 7:3 to ensure the representativeness and randomness of the sample distribution. In addition, 55 cases of MM samples in the GSE57317 dataset were collected from the Gene Expression Omnibus (GEO, https://www.ncbi.nlm.nih.gov/geo/) database. Importantly, genes related to PCD were obtained from a previous study [12].

Preprocessing of RNA-seq data for TCGA

1) Eliminating samples without clinical follow-up data;

2) Retaining samples with a survival time longer than or equal to thirty days;

3) Eliminating samples without survival state;

4) Gene Symbol Conversion from Ensembl;

5) The median was used to normalize the gene with numerous gene symbols.

GEO data preprocessing

After downloading the standardized microarray probe expression data (GSE57317), the probe expression was transformed into gene expression using the platform annotation file. The average expression of several probes corresponding to the same gene was used as the expression value of the gene, while the probes were eliminated when only one probe matched several genes. The maximum expression value was taken when more than one probe matched to the same gene. MM specimens were removed, and patients in good survival status with a survival time longer than 30 days were included in this analysis. Finally, 55 MM samples in GSE57317 were kept.

Identification of molecular subtypes using PCD-related genes

Unsupervised clustering is a data mining approach that uses only internal attributes to identify unknown clusters of potential objects. Consensus clustering (CC) uses repeated subsampling and clustering to produce quantitative and graphical "stability" proof. Specifically, ConsensusClusterPlus extends the CC algorithm by initially subsampling a specific percentage of items and a specific percentage of features in the data matrix. A user-specified clustering method then splits each subsample into several categories [21]. This study

applied CC to classify the molecular subtypes in the "ConsensusClusterPlus" R program [21]. The 500 bootstraps were conducted utilizing the "km" algorithm and "1 - Spearman correlation" as a metric distance. Each bootstrap included 80% of the training set of patients. The optimal subtype was determined by consistent cumulative distribution function, and the number of clusters was between two and ten.

Association between molecular subtypes and immune properties

The correlation between immune checkpoint genes in different molecular subtypes was analyzed. A total of 67 immune checkpoint genes taken from early research were included as the representative immune checkpoints [22]. Using Kruskal, the levels of immune checkpoint gene expression in the molecular subtypes were assessed. Tumor immune dysfunction and exclusion (TIDE) algorithm was employed to evaluate potential responses of MM patients to immune checkpoint blockade (ICB) [23]. Specifically, differences in T-cell rejection characteristics in different MM molecular subtypes were further compared based on the gene expression profiles of dysfunction, exclusion, tumor-associated macrophage M2 types (TAM.M2), myeloid-derived suppressor cell (MDSC), and cancer-associated fibroblast (CAF) using TIDE software [23, 24].

Functional enrichment analysis

Single-sample GSEA (ssGSEA) [25] refers to the absolute enrichment of a gene set in each sample from a dataset. Here, the R package "GSVA" [26] was used to calculate the scores of the 34 biological pathways to obtain ssGSEA scores for each sample. Furthermore, based on the HALLMARK gene set in the Molecular Signatures Database (MSigDB, http://software.broadinstitute.org/gsea/msigdb) [27], we performed GSEA pathway analyses to identify unique biological processes and evaluate differentially activated pathways across the molecular subtypes.

Development of a PCD-related prognostic model

Differentially expressed genes (DEGs) from previously identified molecular subtypes were screened by the R package "limma" [28], and those with |logfc|>log2(1.5) and p<0.05 in each molecular subtype were extracted. Moreover, we employed one-way Cox regression analysis to screen genes with differential expression and utilized the "survival" R package to identify multiple important PCD-related features (p<0.05) [29]. Next, the R package "glmnet" was utilized to further limit the number of genes, and the prognostically relevant genes were determined by LASSO regression [30]. Next, the

Risk score for the MM patients was calculated by the following formula: Risk score = $\Sigma\beta i \times Expi$), where β is the gene Cox regression coefficient and i is the gene expression level. Then the Risk score was subjected to Z-score, and the MM samples of the training set, validation set, and GSE57317 dataset were classified into high-risk group (zscore >0) and low-risk group (zscore <0) by the threshold value of "0". Prognostic analyses were performed by plotting the Kaplan-Meier (KM) survival curves, and significant differences were assessed by log-rank test. Furthermore, receiver operating characteristic (ROC) curves were plotted and 1-, 2-, and 3-year area under the curve (AUC) was computed using the R package "timeROC" [31].

Correlation analysis between Risk scores and drug sensitivity

Based on in the Genomics of Drug Sensitivity in Cancer (GDSC) database, the sensitivity of MM patients to several drugs was predicted using the "oncPredict" package [32] in R software. In addition, the IC_{50} values of drugs for samples from the MMRF-COMPASS training set cohort was also calculated. Further, the correlation between drug sensitivity and Risk score was predicted using Pearson correlation analysis, with p<0.05 and |cor|>0.3 being considered as statistically significant.

Statistical analysis

R program (v4.2.1) was used to conduct statistical analysis. The Student t-test or Wilcoxon test was used to compare the two groups. The Kruskal-Wallis one-way ANOVA was applied to assess the comparisons between two or more groups. We plotted Kaplan-Meier survival curves and evaluated the variations between the curves. Correlation analysis between continuous variables was performed using Spearman's rank correlation. P-value of 0.05 served as the cutoff for statistical significance in all analyses. Ns represented $p > 0.05$; *$p < 0.05$, **$p < 0.01$, ***$p < 0.001$, and ****$p < 0.0001$.

RESULTS

Identification of molecular subtypes using prognostically relevant PCD genes for MM

The association between the expression of PCD-related genes in the MMRF-COMPASS training set cohort patients was analyzed. Here, a total of 434 genes significantly related to the prognosis of MM were filtered (p<0,001). Subsequently, according to the expression profiles of the 434 genes, 592 patients in MMRF-COMPASS training cohort were classified by consensus clustering method. From the results of the

cumulative distribution function (CDF) Delta area, the CDF downward slope was the smallest at k = 6, which had a more stable clustering result (Supplementary Figure 1). Therefore, the whole cohort was divided into six molecular subtypes (C1, C2, C3, C4, C5, C6) (Figure 1A) with significant prognostic differences (Figure 1B). Overall, MM patients in the C5 subtype had a better prognosis, in contrast, those in the C6 subtype had a lower survival rate. Figure 1C shows the distinct clinical features of MM patients in the six subtypes, and it can be observed that most patients in the C1, C3, and C6 subtypes did not differ significantly in terms of their staging, grading, and age. Meanwhile, the results of differential analysis demonstrated significant differences between different PCD scores across the six molecular subtypes (Figure 1D). Subsequently, analysis on the clinicopathological features between different subtypes in the MMRF-COMPASS training cohort showed a higher grade of the C6 subtype (Figure 1E). Overall, MM prognosis and the expression of PCD-related genes were remarkably different among the six molecular subtypes.

Association between the molecular subtypes and immunotherapy

Considering the efficacy of ICB in cancer immunotherapy, we assessed the differential expression of a representative set of 67 immune checkpoint genes from a previous study [22] among the six molecular subtypes. As shown in Figure 2A, most of the immunosuppressive, immune-activating and TwoSide genes were upregulated in the C4 and C6 subtypes but downregulated in the C1 and C5 subtypes. Additionally, significant differences in the expression of the four immune checkpoint genes (*TIGIT*, *CTLA4*, *CD274* and *BTLA)* were observed among the six molecular subtypes, with *BTLA* having a high expression and TIGIT and *CTLA4* having a low expression (Figure 2B). These results indicated that the expression pattern of the immune checkpoint genes could be considered as a marker for evaluating the immunotherapy responses of MM patients.

Subsequently, it was found that the infiltration abundance of MDSC, CAF and TAM differed
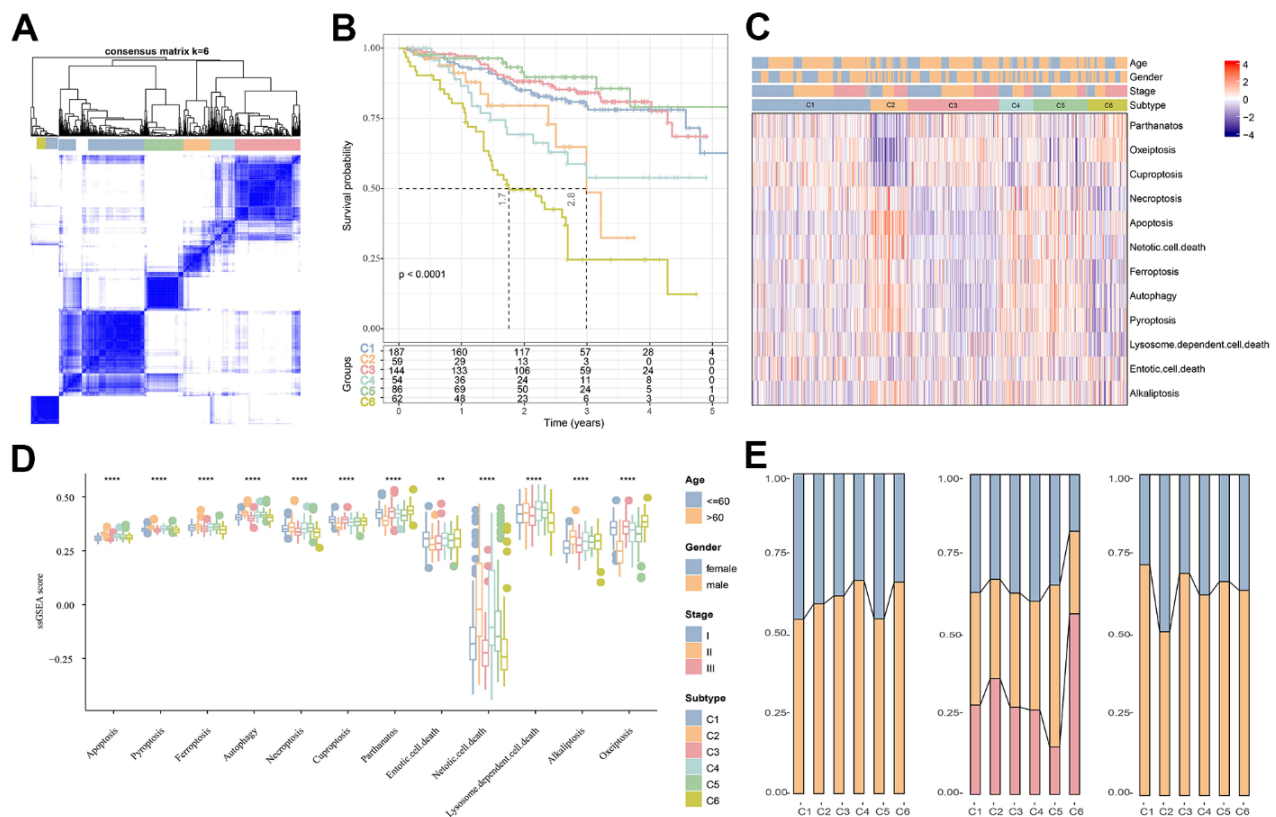
Figure 1. Cluster analysis of different subtypes of MM based on PCD-related genes. (**A**) Heatmap of sample clustering in MMRF-COMPASS with a total of k = 6. (**B**) Relationship KM curves of OS prognosis for six molecular subtypes. (**C**) Differences in PCD between molecular subtypes in the MMRF-COMPASS cohort. (**D**) Heat map of statistically significant different PCD levels in different subtypes. (**E**) Clinicopathological characteristics of the six molecular subtypes in the MMRF-COMPASS training cohort. **p < 0.01, ****p < 0.0001.

significantly across the molecular subtypes, specifically, these three types of cells showed a higher infiltration in C6, C5, and C2, respectively. TIDE analysis also showed that the TIDE score was higher in C6 subtype (Figure 2C). The high exclusion score in the C6 subtype indicated that this subtype evaded the immune system mainly through immune exclusion mechanisms, whereas a high dysfunction score in the C5 subtype indicated that MM patients in this subtype relied on immune cell dysfunction for immune escape. This suggested that different subtypes of MM tumors required different immunotherapeutic strategies to respond effectively.

Characterization of the pathways for the six molecular subtypes of MM

Using the HALLMARK gene set from the MSigDB database, GSEA was employed to identify differentially activated pathways in the six molecular subtypes of MM, with FDR<0.05 showing a significant enrichment. The analysis revealed that pathways such as oxidative phosphorylation and DNA repair were activated in the C3 subtype and apoptosis-related pathways were more activated in the C2 and C4 subtypes, whereas most signaling pathways appeared to be relatively stable in the C1, C5 and C6 subtypes (Figure 3).
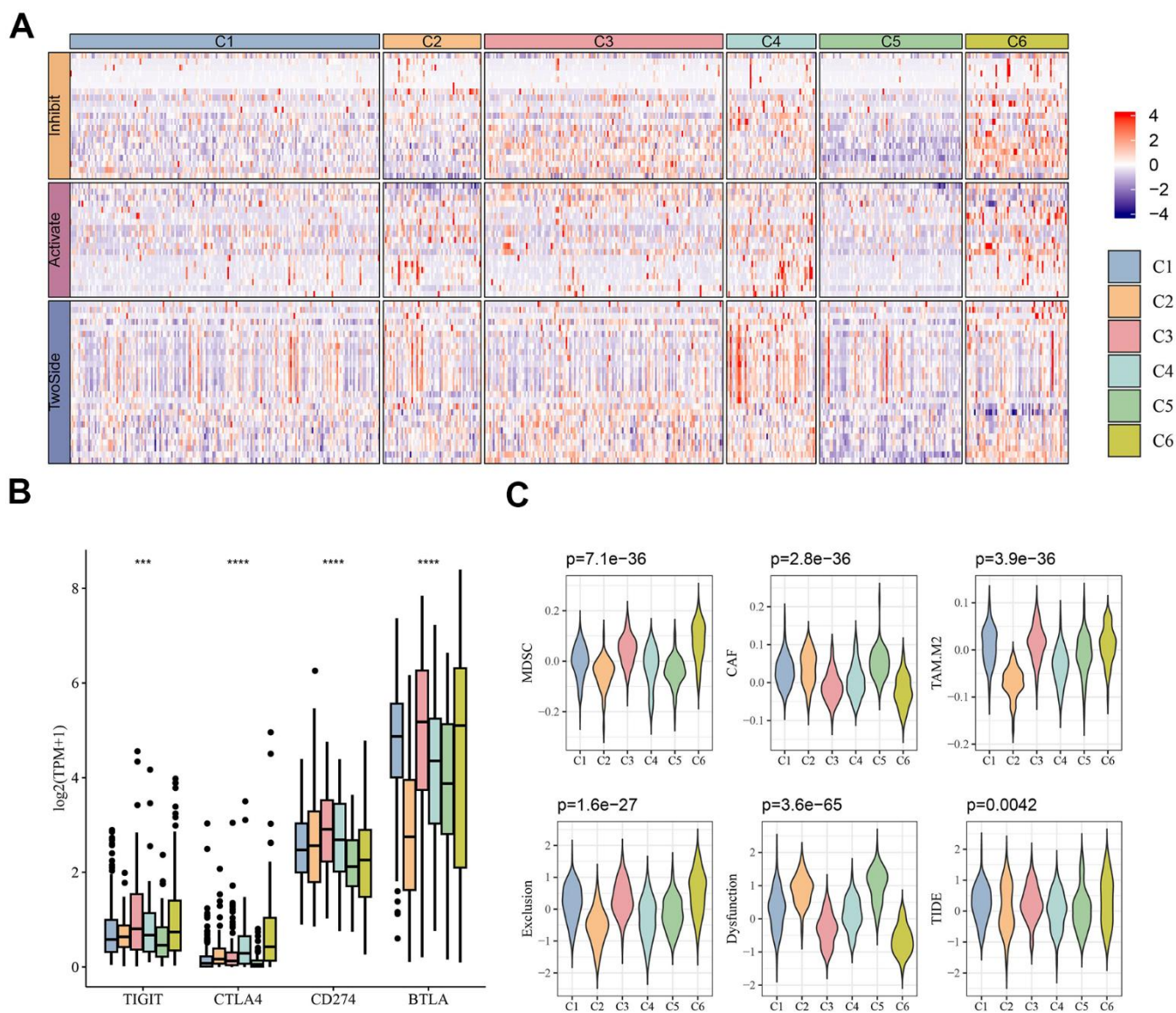
Figure 2. Immunotherapy analysis. (**A**) Heatmap of expression of immune checkpoint genes between different molecular subtypes. (**B**) Differential expression of common immune checkpoint genes *TIGIT*, *CTLA4*, *CD274* and *BTLA* between different molecular subtypes. (**C**) Results predicted by TIDE software. ***$p < 0.001$, ****$p < 0.0001$.

In addition, we further identified DEGs by comparing each subtype against other subtypes (e.g., C1 vs. all others, C2 vs. all others, etc.) using the 'limma' package under the criteria of FDR < 0.05 and |log2FC| > log2(1.5) (Figure 3B). Moreover, analysis on the distribution of DEGs across these molecular subtypes showed that only eight genes were consistently differentially expressed in all the subtype comparisons (C1 vs. others, C2 vs. others, C3 vs. others, C4 vs. others, C5 vs. others, and C6 vs. others) (Figure 3C). Collectively, these findings indicated that different subtypes of MM were characterized by specific genomic and molecular features, which were closely correlated with MM prognosis.

Development and validation of a clinical predictive model

Previous analyses identified the DEGs across the six subtypes of MM using the 'limma' package. Subsequently, 7035 genes that significantly influenced the prognosis of MM patients were screened by univariate Cox regression analysis and further subjected to LASSO regression using the R package "glmnet" to compress the gene number. As shown in Figure 4A, the number of independent variables whose coefficients tended to zero went up with the gradual increase of lambda. We employed 3-fold cross-validation for the model development and analyzed the confidence
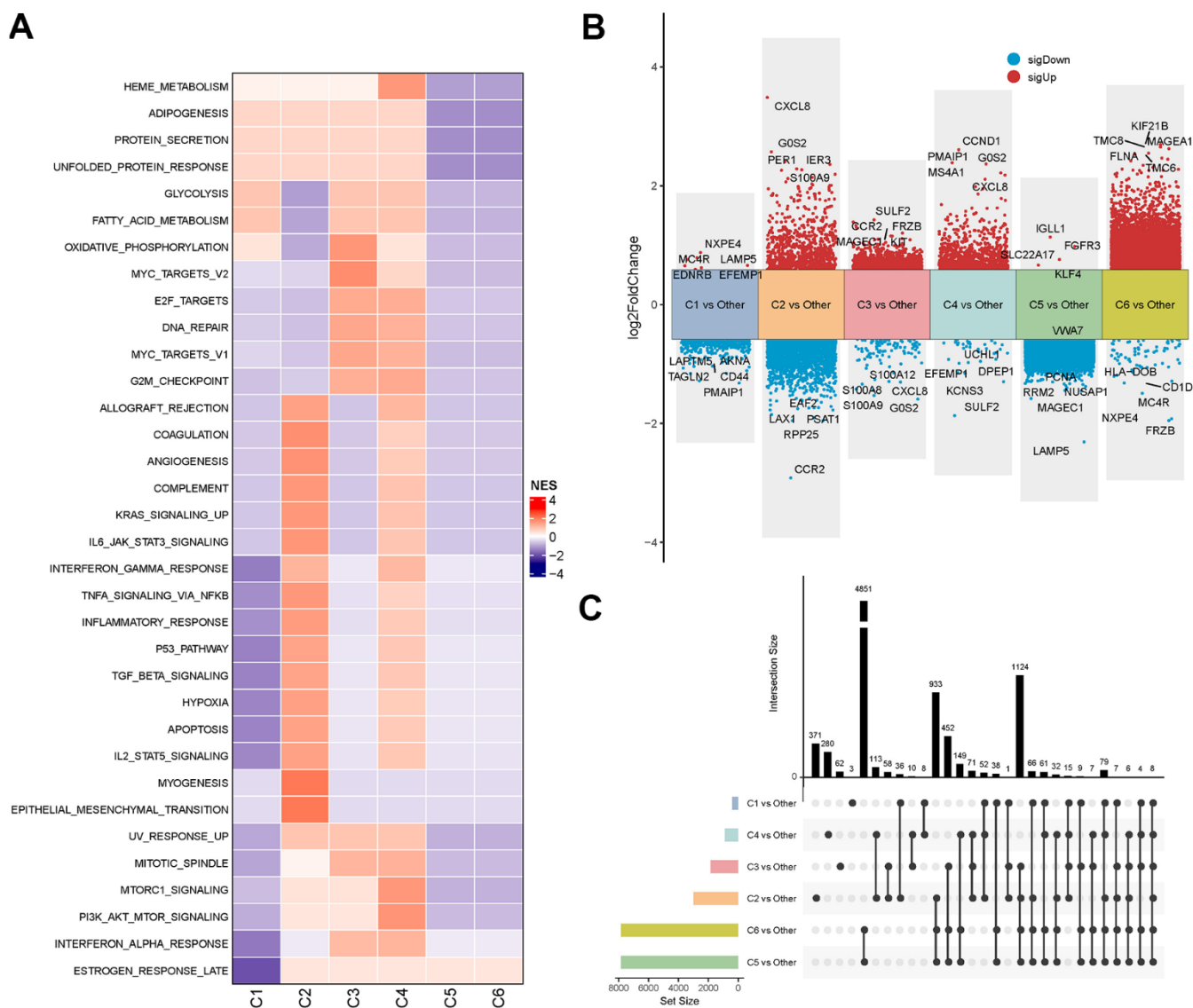
Figure 3. Signalling and genomic landscapes between different subtypes in the MMRF-COMPASS training cohort. (**A**) Signaling pathway activities of different molecular subtypes in the MMRF-COMPASS training cohort. Results of differential expression analysis (**B**) and distribution (**C**) of genes between molecular subtypes in the MMRF-COMPASS training cohort.

intervals under each lambda (Figure 4A). The model was the optimal when lambda=0.0539, under which a total of 24 genes were selected as the target genes for subsequent analysis. Then, using the 24 genes in the LASSO analysis, we conducted stepwise multivariate regression analysis and used the stepAIC method in the MASS package. Starting with the most complex model, one variable was removed iteratively at a time to reduce the AIC. Through this process, we finally identified 12 genes, namely, *HMGB3*, *IL24*,

CD38, *GZMB*, *RHOC*, *CEACAM1*, *FABP5*, *HPDL*, *SHROOM3*, *WNT9A*, *FOXD1*, and *TJP1* (Figure 4B–4C).

Each patient in the TCGA cohort was assigned with a Risk score calculated by the formula: Risk score=0.178* *HMGB3*+0.185**IL24*-0.303**CD38*+0.219**GZMB*+0.193**RHOC*-0.141**CEACAM1*+0.186* *FABP5*+ 0.213* *HPDL*+ 0.125**SHROOM3*+ 0.233**WNT9A*+ 0.213* *FOXD1*-0.097**TJP1*.
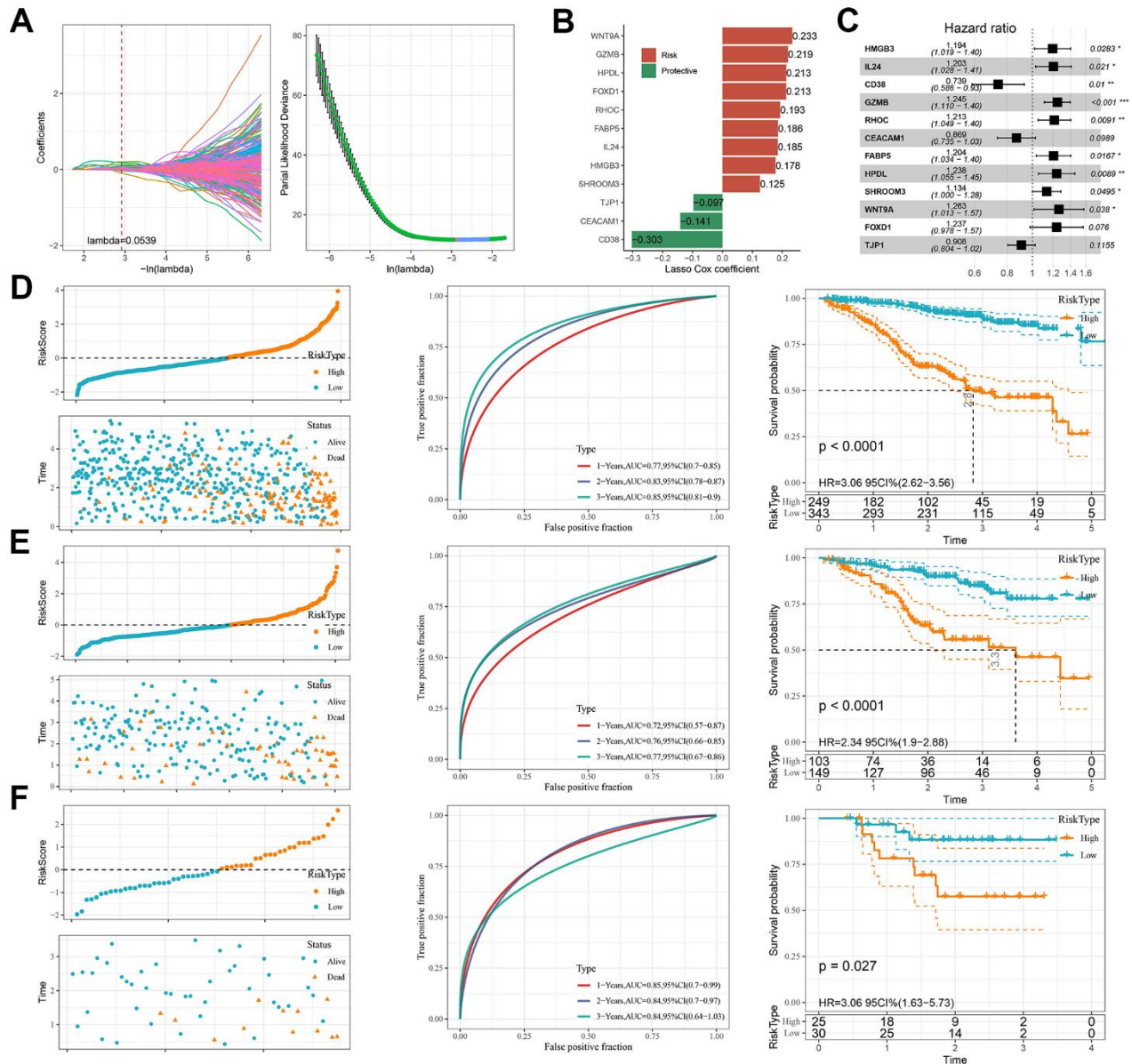
Figure 4. PCD-based risk model construction and validation. (**A**) Trajectories of each independent variable with lambda and confidence intervals under lambda. (**B**) Key genes of the prognostic model. (**C**) Forest plot of key genes of the prognostic model. (**D**–**F**) Validation of clinical prognostic models for the MMRF-COMPASS training set cohort, MMRF-COMPASS validation set cohort, and GSE57317 cohort, respectively. They are, from left to right: Risk score, survival time versus survival status and expression of prognostic genes, KM Survival Curve Distribution, and ROC Curve.

Next, we compared the survival time of MM patients in different subgroups and found that high-risk patients had shorter survival time than low-risk patients ($p < 0.0001$). Moreover, the AUC values for 1-, 2-, and 3- year survival reached 0.77, 0.83, and 0.85, respectively (Figure 4D). Notably, similar results in the MMRF-COMPASS validation set cohort ($p < 0.0001$) and the GSE57317 cohort ($p = 0.027$) were observed, with high-risk patients showing a significantly worse OS. The AUC values for 1-, 2-, and 3- year survival prediction in the MMRF-COMPASS validation set cohort reached 0.72, 0.76 and 0.77, respectively ($p < 0.0001$, Figure 4E). In GSE57317 cohort, the AUC values for 1-, 2-, and 3- year survival prediction were 0.85, 0.84 and 0.84, respectively ($p < 0.05$, Figure 4F). These results

demonstrated robust prognostic predictability of PCD-related genes.

Establishment and assessment of a nomogram

Subsequently, differences in clinicopathological features between the risk subgroups in the MMRF-COMPASS training set were compared. It was found that gender and age did not differ significantly between the two risk groups, whereas the Risk score increased as the clinical grade advanced (Figure 5A). We further performed multivariate Cox regression analysis combining stage, age, gender, and the Risk score to establish a nomogram to better evaluate OS for MM patients. As shown in Figure 5B, the Risk score showed the greatest impact on the OS prediction in
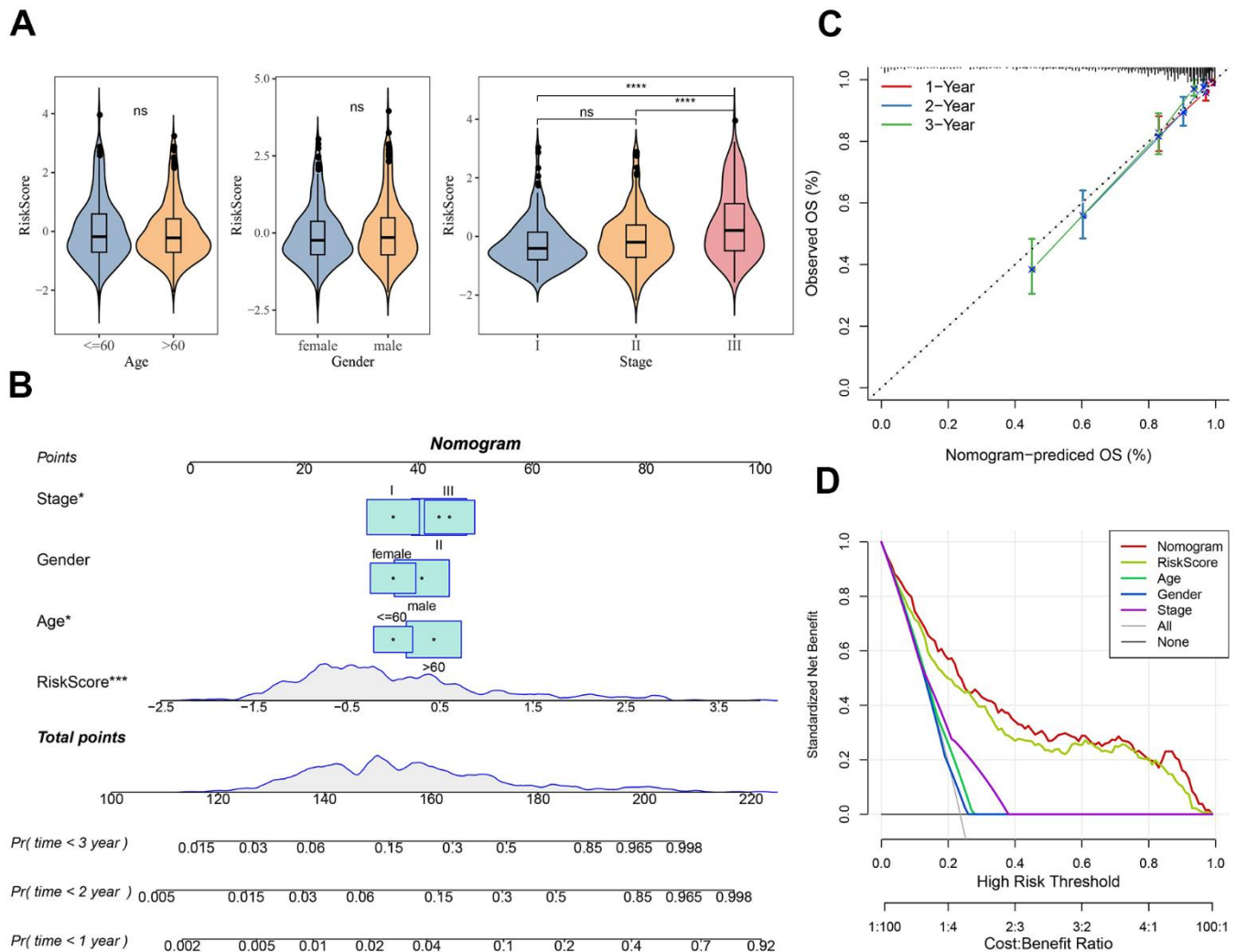
Figure 5. Nomogram construction for predicting the prognosis of MM patients. (**A**) Differences in clinicopathological characteristics between risk subgroups in the MMRF-COMPASS training set. (**B**) Risk score combines clinical features to create column-line plots. (**C**) Calibration curves were used to validate the established column line plots. (**D**) Decision curve analysis of column-line plots. Ns represents $p > 0.05$, and ****$p < 0.0001$.

MM, followed by age and stage. Further, the calibration curves demonstrated that the 1-, 2-, and 3-year prediction calibration curves were close to the standard ones, suggesting that the model had a high prediction accuracy (Figure 5C). Interestingly, the accuracy of our risk model further assessed by the decision curve analysis (DCA) also performed well in assessing MM prognosis. (Figure 5D).

Enrichment pathway analysis and drug sensitivity assessment for MM patients in different risk groups

Subsequently, we calculated ssGSEA scores for each sample based on the HALLMARK Pathway and used Wilcoxon rank-sum test to identify differential pathways between the two risk groups of MM. Pathways such as hypoxia, angiogenesis and apoptosis were notably activated in the high-risk group, whereas pathways including NOTCH_SIGNALING and KRAS_SIGNALING_DN were more activated in the low-risk group (Figure 6A). After calculating the IC_{50} values for

each drug in the MMRF-COMPASS training set cohort, a significant correlation (FDR<0.05 and |cor|>0.3) between nine drugs and the Risk score was detected. Analysis on the correlation between the Risk score, the expression of key model genes and the IC_{50} values of the drugs revealed that MM patients in the high-risk group had a higher IC_{50} values for the drug SB505124_1194 (Figure 6B, 6C), suggesting that MM patients with higher Risk score value might be resistant to SB505124_1194 (p=3.7e-22). Similarly, patients in the low-risk group may be resistant to AZD7762_1022 (p=1e-20). Thus, SB505124_1194 and AZD7762_1022 were considered as valid references for evaluating chemotherapy resistance in MM patients.

DISCUSSION

Due to drug resistance and surgical recurrence, MM as the second most common hematological malignancy is largely incurable [33]. Study confirmed that PCD is crucially involved in carcinogenesis, immunological
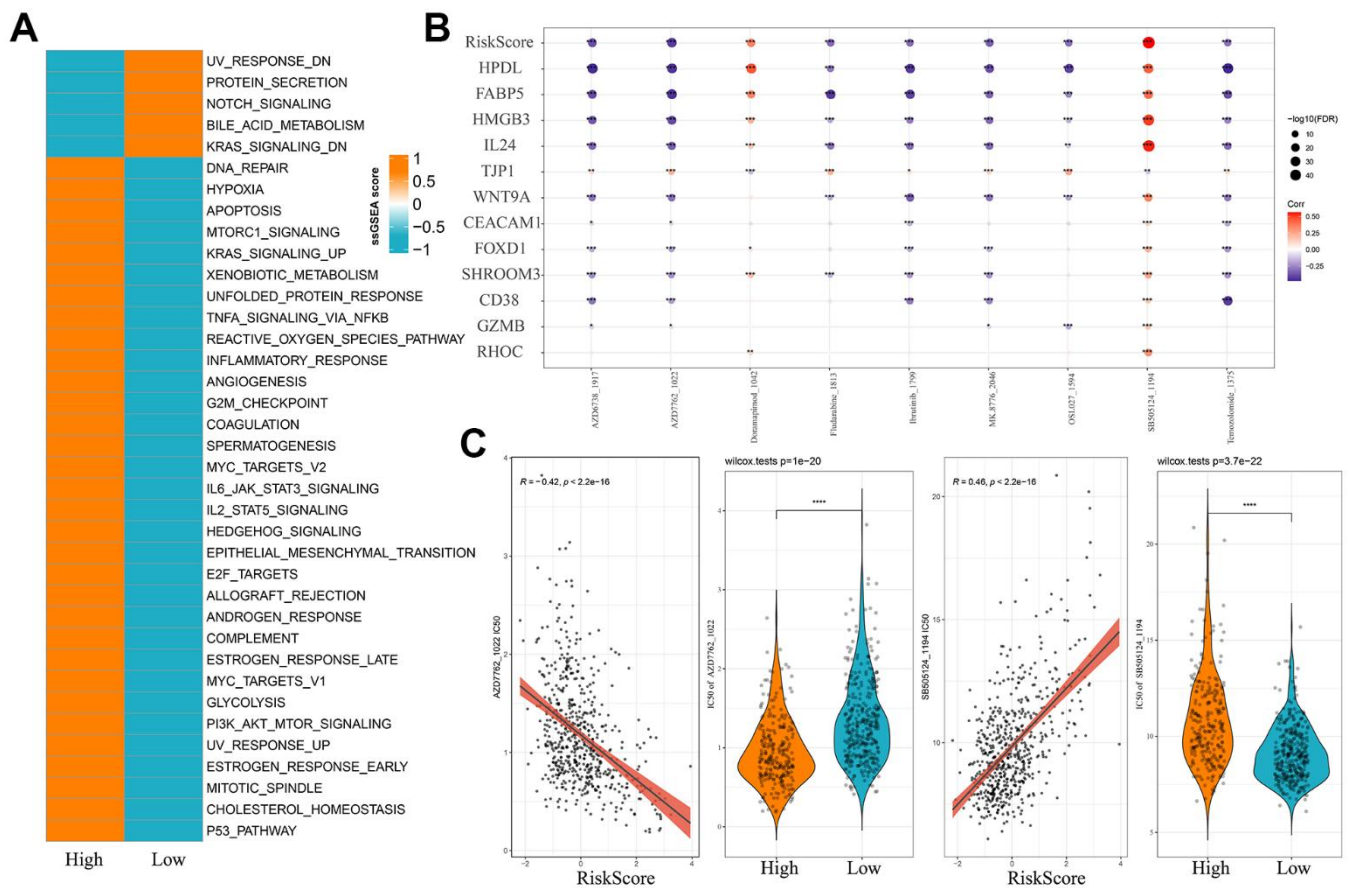
Figure 6. Risk models and pathway characteristics and drug sensitivity differ between patients in different MM risk groups. (**A**) HALLMARK pathway differences between high and low-risk subgroups. (**B**) Bubble plots of Risk score in the MMRF-COMPASS training set cohort and expression of key genes in the model versus drug IC_{50} values, size and color indicate the strength of the association. (**C**) Comparison of IC_{50} scores versus drugs between high and low-risk groups. *p < 0.05, **p < 0.01, ***p < 0.001, and ****p < 0.0001.

infiltration, progression, prognosis, and treatment effectiveness of cancers [34, 35]. For example, Zou et al. [12] developed a PCD signature based on immune checkpoint genes to evaluate the prognosis and drug sensitivity for patients with triple-negative breast cancer. Similarly, Qin et al. [36] discovered 16 PCD genes that are highly effective in predicting the prognosis and immunotherapy response for patients with oesophageal squamous cell carcinoma. Additionally, a significant correlation between PCD and immune features, including immune cell infiltration and the expressions of immune checkpoint molecules, has also been found in lung adenocarcinoma [37]. At present, the study of PCD in MM is largely limited to individual form of PCD, such as apoptosis [38], ferroptosis [39], autophagy [40] and cuproptosis [41]. However, different PCD forms are not necessarily mutually exclusive. Numerous redundancies and crosstalk have been observed in signaling pathways that regulate these patterns of cell death, suggesting that they may work together to influence tumorigenesis and tumor progression [42]. Therefore, using predictive features that integrate information from multiple PCDs may better characterize tumor status. This study analyzed the integrated landscape of PCD in the context of translational medicine, aiming to improve the understanding of the role of PCD in MM.

The TME and its components provide the foundation for the proliferation and survival of malignant cells [43]. The TME is also involved in checkpoint blockade immunotherapy and immunosuppression [44]. According to previous reports, immunosuppressive cell infiltration in the TME is a key marker of the immune microenvironment in tumors, significantly influencing the development of malignancies. Pro-tumourigenic immune cells are attracted by CAF to prevent pro-tumourigenic CD8+T cell infiltration [45]. Furthermore, in addition to impeding the invasion of immune cells, MDSC in the TME can directly bind to immune checkpoint receptors on tumor cells, blocking the oncogenic effects of T cells [46]. Similarly, TAM infiltration in TME is related to treatment resistance, metastasis, and immunosuppression in the majority of malignancies [47]. It has been demonstrated that immunological failure in MM patients is associated with the infiltration of immunosuppressive cells, and that the immunosuppressive mediators of these cells are correlated with the prognosis of patients [48, 49]. In the present study, high MDSC infiltration in the C6 subtype may have a suppressive effect on immune cell functions and this was correlated with high rejection scores in the subtype, suggesting that MDSC may evade the immune system mainly through immune rejection mechanisms. Similarly, high CAF infiltration in the C5 subtype was associated with a high dysfunction score, indicating that

CAF cells may rely on immune cell dysfunction for immune escape. In addition, macrophage infiltration could also induce immune suppression. Patients with higher TIDE scores have shown a higher likelihood of immune escape and less active response to immune checkpoint inhibitors (ICI) therapy [23]. Overall, TAM, MDSC and CAF cell infiltration in the TME may be the main cause of immune escape in MM patients.

Immune checkpoints could preserve the balance in the body and inhibit abnormal immune response activation. Tumor cells, however, avoid immune response by taking advantage of this feature of immune checkpoint molecules [50]. Immune checkpoint blockade (ICB) therapy has attracted much research interest and demonstrated promising outcomes in cancer treatment [51]. The immunoglobulin-associated receptor family (*TIGIT*, *CTLA4*, *CD274*, and *BTLA*) have inhibitory effects on T cell function and have been used as a part of immunomodulatory strategy for treating cancers [52]. Study reported that high-expressed *CTLA4* and *CD274* in head and neck squamous cell carcinoma (HNSCC) may cause immune dysfunction in the patients [53]. In addition, Hong et al. also found a positive link between the expression level of *BTLA* and that of *TIGIT* in renal cell carcinoma, showing the potential to be considered as a pair of targets in the immunotherapy for the tumor [54]. It was found that dysregulated expression of immune checkpoints may account for a lower clinical response to immune checkpoint therapy in MM [55]. Here, we found significant differences in the expression of *TIGIT*, *CTLA4*, *CD274* and *BTLA* among all the six molecular subtypes. Notably, *BTLA* had higher expression levels in these molecular subtypes, suggesting that immune checkpoint therapy blocking BTLA may have better efficacy to MM patients in different subtypes.

To further improve the clinical applicability, we identified 12 PCD-related genes that affected the prognosis of MM using stepwise regression analysis, including *HMGB3*, *IL24*, *CD38*, *GZMB*, *RHOC*, *CEACAM1*, *FABP5*, *HPDL*, *SHROOM3*, *WNT9A*, *FOXD1*, and *TJP1*. *HMGB3* could regulate breast cancer cell autophagy and apoptosis, promoting cell migration, invasion and metastatic potential [56]. *IL24* inhibits MM cell tumor growth by inducing tumor cell autophagy, thus suppressing MM cell tumor growth [57]. The transmembrane glycoprotein *CD38* mediates T-cell activation and has an immunomodulatory effect on the TME in MM [58]. Although, CD38 expression is commonly increased in MM, it is present as a tumor suppressor in HNSCC [59]. This phenomenon may be related to the drug resistance of the samples selected in this study, which requires further validation. *GZMB* has been reported to serve as an immune response regulator in the immune activation of

artificial pluripotent stem cells in MM [60]. Li et al. [61] observed that *GZMB* hinders immune evasion by inducing pyroptosis and apoptosis in acute myeloid leukemia (AML) cells. In addition, *RHOC*, a ferroptosis and cuproptosis-related gene that affects the prognosis of AML, has a strong ability in predicting the OS of the cancer [62]. *RHOC* can promote tumor growth and induce tumor angiogenesis in MM [63]. In addition, *CEACAM1* plays an oncogenic role in MM by inhibiting tumor cell proliferation, invasion and migration, and inducing apoptosis [64]. The lipid chaperone protein *FABP5* promotes cell proliferation, inhibits apoptosis and enhances chemotherapy resistance in MM patients [4, 65]. High expression of *HPDL* in pancreatic ductal adenocarcinoma is predictive of poorer prognosis and immunosuppression in the patients [66]. In addition, bioinformatics analysis revealed that *SHROOM3* is a strong predictor of prognosis, immune activity, and treatment response of clear cell renal cell carcinoma [67]. Previous research verified that the mRNA expression level of *WNT9A* is significantly associated with the biochemical recurrence of prostate cancer [68]. *FOXD1* could be able to promote cell proliferation and inhibit apoptosis by regulating polo-like kinase 2 in colorectal cancer [69]. Another study reported that *TJP1*, whose expression is low in MM, inhibits tumor metastasis by increasing the adhesion of MM cells to bone marrow stroma [70]. These results suggested that most of these genes were associated with the development of one or more PCD forms in tumors, and that their different roles in tumors may be related to the TME. In accordance with the available analyses, these genes were largely linked to cell invasion and metastasis, immune infiltration and therapeutic response, which was of important value in the prognostic prediction in MM.

Subsequently, we identified differential pathways between high- and low-risk groups, and found that pathways such as hypoxia and angiogenesis, which were closely related to tumor development and progression, were remarkably activated in the high-risk group [71]. The activation of the apoptotic pathway once again proved the anti-tumor effect of *CEACAM1* in MM [64]. In the low-risk group, pathways such as NOTCH_SIGNALING and KRAS_SIGNALING_DN were more activated, indicating that the bone marrow microenvironment of low-risk MM patients may be an ideal microenvironment for the proliferation and migration of MM cells [72–74]. These results suggested that differences in tumor behaviors in different subgroups of MM may be a result of aberrant activation of different genes and pathways, which was a crucial cause leading to tumor progression and a key clinical target. The therapeutic efficacy of post-surgical adjuvant chemotherapy in treating most tumors has been widely recognized [75]. However, the

heterogeneity of the TME may cause resistance and different responses to the therapy in different patients [8]. Similarly, improving drug resistance in MM patients could contribute to a better prognosis of the patients. Therefore, we developed a risk model with the sensitivity to several most commonly used drugs in MM therapies. Higher IC_{50} values of SB505124_1194 in the high-risk group may explain the unfavorable prognostic outcomes in this group. The anticancer sensitivity of the drug predicted by ferroptosis-related genes has also been verified in AML [76]. AZD7762 could enhance tumor cell sensitivity to DNA damage and cisplatin-induced apoptosis in osteosarcoma cells [77]. Considering the fact that low-risk MM patients may be resistant to AZD7762_1022, it can be speculated that MM patients could respond to most PCD-related chemotherapeutic agents. These findings supported that the Risk score developed with the PCD genes contributed to the clinical management of MM patients.

However, there were certain limitations in this study to be noted. Firstly, bias may be unavoidably caused by the retrospective recruitment of patients. Secondly, additional experimental research is required to analyze the biological roles of some PCD genes that have not been investigated in MM cells. Furthermore, this study only assessed the sensitivity of MM to two different types of medications applying bioinformatics analysis, therefore tissue tests are needed to confirm the validity of the current results. Finally, multicenter randomized controlled studies with large sample sizes and follow-up data are also encouraged to be carried out for further validation.

CONCLUSIONS

In this study, six molecular subtypes of MM were identified using PCD genes, which can be employed to characterize different prognostic and immune states of MM patients. In addition, a robust 12-gene Risk score model developed based on the differential genes were independent of clinicopathological characteristics and showed stable prediction performance in both independent datasets. Moreover, the model could be applied to assess the sensitivity of MM patients to anticancer drugs. This helped to better understand the mechanism through which PCD influenced the progression of MM and also provided a theoretical reference for the clinical targeted therapy of MM.

Abbreviations

MM: Multiple myeloma; PCD: Programmed cell death; MsigDB: Molecular signatures database; RNA-seq: Transcriptome sequencing; KEGG: Kyoto encyclopedia of genes and genomes; CC: Consensus clustering; CTL:

Tumour-infiltrating cytotoxic T lymphocyte; CAF: Tumour-associated fibroblasts; TAM: M2 subtype tumour-associated macrophage; MDSC: Myeloid-derived suppressor cells; KM: Kaplan-Meier; GDSC: Drug Sensitivity in Cancer; IC50: Inhibitory concentration; AUC: Area under ROC curve; DCA: Decision curve analysis; GEO: Gene Expression Omnibus; LASSO: Least Absolute Shrinkage and Selection Operator; OS: Overall Survival; ROC: Receiver Operating Characteristic analysis; GSVA: Gene Set Variant analysis; ssGSEA: single-sample gene set enrichment analysis; TCGA: The Cancer Genome Atlas; TIDE: Tumor Immune Dysfunction and Exclusion; ICIs: Immune Checkpoint Inhibitors.

AUTHOR CONTRIBUTIONS

All authors contributed to this present work: [YL], [HBZ] and [ZWJ] designed the study, [XYL] and [GRC] acquired the data, [TJQ], [FXW] and [XYK] interpreted the data. [YL], [HBZ], [XYK] and [ZWJ] drafted the manuscript, [YL], [TJQ], [XYL] and [GRC] revised the manuscript. All authors read and approved the manuscript.

CONFLICTS OF INTEREST

The authors declare that they have no known competing financial interests or personal relationships that could have appeared to influence the work reported in this paper.

FUNDING

REFERENCES

1. van de Donk NW, Pawlyn C, Yong KL. Multiple myeloma. Lancet. 2021; 397:410–27. https://doi.org/10.1016/S0140-6736(21)00135-5 PMID:33516340

2. Kumar SK, Rajkumar V, Kyle RA, van Duin M, Sonneveld P, Mateos MV, Gay F, Anderson KC. Multiple myeloma. Nat Rev Dis Primers. 2017; 3:17046. https://doi.org/10.1038/nrdp.2017.46 PMID:28726797

3. Zhang X, Zhou Z, Wang J, Han M, Liu HAN, Zang M. Immune checkpoint receptors and their ligands on CD8 T cells and myeloma cells in extramedullary multiple myeloma. Biocell. 2024; 48:303–11.

4. Farrell M, Fairfield H, Karam M, D'Amico A, Murphy CS, Falank C, Pistofidi RS, Cao A, Marinac CR, Dragon JA, McGuinness L, Gartner CG, Iorio RD, et al. Targeting the fatty acid binding proteins disrupts multiple myeloma cell cycle progression and MYC signaling. Elife. 2023; 12:e81184. https://doi.org/10.7554/eLife.81184 PMID:36880649

5. Lu Q, Yang D, Li H, Niu T, Tong A. Multiple myeloma: signaling pathways and targeted therapy. Mol Biomed. 2024; 5:25. https://doi.org/10.1186/s43556-024-00188-w PMID:38961036

6. Bird S, Pawlyn C. IMiD resistance in multiple myeloma: current understanding of the underpinning biology and clinical impact. Blood. 2023; 142:131–40. https://doi.org/10.1182/blood.2023019637 PMID:36929172

7. Kim K, Phelps MA. Clinical Pharmacokinetics and Pharmacodynamics of Daratumumab. Clin Pharmacokinet. 2023; 62:789–806. https://doi.org/10.1007/s40262-023-01240-8 PMID:37129750

8. Kazmi SM, Nusrat M, Gunaydin H, Cornelison AM, Shah N, Kebriaei P, Nieto Y, Parmar S, Popat UR, Oran B, Shah JJ, Orlowski RZ, Champlin RE, et al. Outcomes Among High-Risk and Standard-Risk Multiple Myeloma Patients Treated With High-Dose Chemotherapy and Autologous Hematopoietic Stem-Cell Transplantation. Clin Lymphoma Myeloma Leuk. 2015; 15:687–93. https://doi.org/10.1016/j.clml.2015.07.641 PMID:26361647

9. D'Agostino M, Bertamini L, Oliva S, Boccadoro M, Gay F. Pursuing a Curative Approach in Multiple Myeloma: A Review of New Therapeutic Strategies. Cancers (Basel). 2019; 11:2015. https://doi.org/10.3390/cancers11122015 PMID:31847174

10. Liu J, Hong M, Li Y, Chen D, Wu Y, Hu Y. Programmed Cell Death Tunes Tumor Immunity. Front Immunol. 2022; 13:847345. https://doi.org/10.3389/fimmu.2022.847345 PMID:35432318

11. Nisa A, Kipper FC, Panigrahy D, Tiwari S, Kupz A, Subbian S. Different modalities of host cell death and their impact on Mycobacterium tuberculosis infection. Am J Physiol Cell Physiol. 2022; 323:C1444–74. https://doi.org/10.1152/ajpcell.00246.2022 PMID:36189975

12. Zou Y, Xie J, Zheng S, Liu W, Tang Y, Tian W, Deng X, Wu L, Zhang Y, Wong CW, Tan D, Liu Q, Xie X. Leveraging diverse cell-death patterns to predict the prognosis and drug sensitivity of triple-negative breast cancer patients after surgery. Int J Surg. 2022; 107:106936.

https://doi.org/10.1016/j.ijsu.2022.106936
PMID:36341760

13. Bedoui S, Herold MJ, Strasser A. Emerging connectivity of programmed cell death pathways and its physiological implications. Nat Rev Mol Cell Biol. 2020; 21:678–95.
https://doi.org/10.1038/s41580-020-0270-8
PMID:32873928

14. Foote HP, Wu H, Balevic SJ, Thompson EJ, Hill KD, Graham EM, Hornik CP, Kumar KR. Using Pharmacokinetic Modeling and Electronic Health Record Data to Predict Clinical and Safety Outcomes after Methylprednisolone Exposure during Cardiopulmonary Bypass in Neonates. Congenit Heart Dis. 2023; 18:295–313.
https://doi.org/10.32604/chd.2023.026262
PMID:37484782

15. Al-Odat OS, Guirguis DA, Schmalbach NK, Yao G, Budak-Alpdogan T, Jonnalagadda SC, Pandey MK. Autophagy and Apoptosis: Current Challenges of Treatment and Drug Resistance in Multiple Myeloma. Int J Mol Sci. 2022; 24:644.
https://doi.org/10.3390/ijms24010644
PMID:36614089

16. Hu D, Wang Y, Shen X, Mao T, Liang X, Wang T, Shen W, Zhuang Y, Ding J. Genetic landscape and clinical significance of cuproptosis-related genes in liver hepatocellular carcinoma. Genes Dis. 2023; 11:516–9.
https://doi.org/10.1016/j.gendis.2023.03.010
PMID:37692498

17. Gu X, Pan J, Li Y, Feng L. A programmed cell death-related gene signature to predict prognosis and therapeutic responses in liver hepatocellular carcinoma. Discov Oncol. 2024; 15:71.
https://doi.org/10.1007/s12672-024-00924-2
PMID:38466483

18. Meng J, Zong C, Wang M, Chen Y, Zhao S. Constructing a Prognostic Model of Uterine Corpus Endometrial Carcinoma and Predicting Drug-Sensitivity Responses Using Programmed Cell Death-Related Pathways. J Cancer. 2024; 15:2948–59.
https://doi.org/10.7150/jca.92201
PMID:38706893

19. Xiao L, He R, Hu K, Song G, Han S, Lin J, Chen Y, Zhang D, Wang W, Peng Y, Zhang J, Yu P. Exploring a specialized programmed-cell death patterns to predict the prognosis and sensitivity of immunotherapy in cutaneous melanoma via machine learning. Apoptosis. 2024; 29:1070–89.
https://doi.org/10.1007/s10495-024-01960-7
PMID:38615305

20. Qin Y, Pu X, Hu D, Yang M. Machine learning-based biomarker screening for acute myeloid leukemia prognosis and therapy from diverse cell-death patterns. Sci Rep. 2024; 14:17874.
https://doi.org/10.1038/s41598-024-68755-3
PMID:39090256

21. Wilkerson MD, Hayes DN. ConsensusClusterPlus: a class discovery tool with confidence assessments and item tracking. Bioinformatics. 2010; 26:1572–3.
https://doi.org/10.1093/bioinformatics/btq170
PMID:20427518

22. Hu FF, Liu CJ, Liu LL, Zhang Q, Guo AY. Expression profile of immune checkpoint genes and their roles in predicting immunotherapy response. Brief Bioinform. 2021; 22:bbaa176.
https://doi.org/10.1093/bib/bbaa176
PMID:32814346

23. Fu J, Li K, Zhang W, Wan C, Zhang J, Jiang P, Liu XS. Large-scale public data reuse to model immunotherapy response and resistance. Genome Med. 2020; 12:21.
https://doi.org/10.1186/s13073-020-0721-z
PMID:32102694

24. Jiang P, Gu S, Pan D, Fu J, Sahu A, Hu X, Li Z, Traugh N, Bu X, Li B, Liu J, Freeman GJ, Brown MA, et al. Signatures of T cell dysfunction and exclusion predict cancer immunotherapy response. Nat Med. 2018; 24:1550–8.
https://doi.org/10.1038/s41591-018-0136-1
PMID:30127393

25. Zhao P, Zhen H, Zhao H, Huang Y, Cao B. Identification of hub genes and potential molecular mechanisms related to radiotherapy sensitivity in rectal cancer based on multiple datasets. J Transl Med. 2023; 21: 176.
https://doi.org/10.1186/s12967-023-04029-2
PMID:36879254

26. Hänzelmann S, Castelo R, Guinney J. GSVA: gene set variation analysis for microarray and RNA-seq data. BMC Bioinformatics. 2013; 14:7.
https://doi.org/10.1186/1471-2105-14-7
PMID:23323831

27. Yu TJ, Ma D, Liu YY, Xiao Y, Gong Y, Jiang YZ, Shao ZM, Hu X, Di GH. Bulk and single-cell transcriptome profiling reveal the metabolic heterogeneity in human breast cancers. Mol Ther. 2021; 29:2350–65.
https://doi.org/10.1016/j.ymthe.2021.03.003
PMID:33677091

28. Ritchie ME, Phipson B, Wu D, Hu Y, Law CW, Shi W, Smyth GK. limma powers differential expression analyses for RNA-sequencing and microarray studies. Nucleic Acids Res. 2015; 43:e47.

https://doi.org/10.1093/nar/gkv007
PMID:25605792

29. Therneau TM, Lumley T. Package ' survival '. 2015.

30. Friedman J, Hastie T, Tibshirani R. Regularization Paths for Generalized Linear Models via Coordinate Descent. J Stat Softw. 2010; 33:1–22.
PMID:20808728

31. Blanche P. timeROC: Time-Dependent ROC Curve and AUC for Censored Survival Data. 2015.

32. Maeser D, Gruener RF, Huang RS. oncoPredict: an R package for predicting *in vivo* or cancer patient drug response and biomarkers from cell line screening data. Brief Bioinform. 2021; 22:bbab260.
https://doi.org/10.1093/bib/bbab260 PMID:34260682

33. Robak P, Drozdz I, Szemraj J, Robak T. Drug resistance in multiple myeloma. Cancer Treat Rev. 2018; 70:199–208.
https://doi.org/10.1016/j.ctrv.2018.09.001
PMID:30245231

34. Hänggi K, Ruffell B. Cell death, therapeutics, and the immune response in cancer. Trends Cancer. 2023; 9:381–96.
https://doi.org/10.1016/j.trecan.2023.02.001
PMID:36841748

35. Su Y, Wang W, Wang Y, Wang C, Sun S, Zhu X, Dai X, Li S, Gao X, Qin K. Application and Development of Targeted Fishing Technology in Natural Product Screening - A Simple Minireview. Current Pharmaceutical Analysis. 2024; 20:231–40.

36. Cao K, Zhu J, Lu M, Zhang J, Yang Y, Ling X, Zhang L, Qi C, Wei S, Zhang Y, Ma J. Analysis of multiple programmed cell death-related prognostic genes and functional validations of necroptosis-associated genes in oesophageal squamous cell carcinoma. EBioMedicine. 2024; 99:104920.
https://doi.org/10.1016/j.ebiom.2023.104920
PMID:38101299

37. Wang S, Wang R, Hu D, Zhang C, Cao P, Huang J. Machine learning reveals diverse cell death patterns in lung adenocarcinoma prognosis and therapy. NPJ Precis Oncol. 2024; 8:49.
https://doi.org/10.1038/s41698-024-00538-5
PMID:38409471

38. Wang H, Shao R, Lu S, Bai S, Fu B, Lai R, Lu Y. Integrative Analysis of a Pyroptosis-Related Signature of Clinical and Biological Value in Multiple Myeloma. Front Oncol. 2022; 12:845074.
https://doi.org/10.3389/fonc.2022.845074
PMID:35296025

39. Wang Q, Zhao M, Zhang T, Zhang B, Zheng Z, Lin Z, Zhou S, Zheng D, Chen Z, Zheng S, Zhang Y, Lin X, Dong R, et al. Comprehensive analysis of ferroptosis-related genes in immune infiltration and prognosis in multiple myeloma. Front Pharmacol. 2023; 14:1203125.
https://doi.org/10.3389/fphar.2023.1203125
PMID:37608887

40. Li L, Chen T, Wang J, Li M, Li Q. Identification of an Autophagy-Related Signature Based on Whole Bone Marrow Sequencing for the Prognosis and Immune Microenvironment Characterization of Multiple Myeloma. J Immunol Res. 2022; 2022:3922739.
https://doi.org/10.1155/2022/3922739
PMID:35677537

41. Li T, Yao L, Hua Y, Wu Q. Comprehensive analysis of prognosis of cuproptosis-related oxidative stress genes in multiple myeloma. Front Genet. 2023; 14:1100170.
https://doi.org/10.3389/fgene.2023.1100170
PMID:37065484

42. Jayadev S, Yusuff I. Robust U-HPLC Method Development of Desonide and its Application to *In Vitro* Release Testing (IVRT) of Topical Cream Products. Current Pharmaceutical Analysis. 2024; 20:327–44.

43. Tajaldini M, Saeedi M, Amiriani T, Amiriani AH, Sedighi S, Mohammad Zadeh F, Dehghan M, Jahanshahi M, Zanjan Ghandian M, Khalili P, Poorkhani AH, Alizadeh AM, Khori V. Cancer-associated fibroblasts (CAFs) and tumor-associated macrophages (TAMs); where do they stand in tumorigenesis and how they can change the face of cancer therapy? Eur J Pharmacol. 2022; 928:175087.
https://doi.org/10.1016/j.ejphar.2022.175087
PMID:35679891

44. Mantovani A, Allavena P, Marchesi F, Garlanda C. Macrophages as tools and targets in cancer therapy. Nat Rev Drug Discov. 2022; 21:799–820.
https://doi.org/10.1038/s41573-022-00520-5
PMID:35974096

45. Chen M, Chen F, Gao Z, Li X, Hu L, Yang S, Zhao S, Song Z. CAFs and T cells interplay: The emergence of a new arena in cancer combat. Biomed Pharmacother. 2024; 177:117045.
https://doi.org/10.1016/j.biopha.2024.117045
PMID:38955088

46. Umansky V, Blattner C, Gebhardt C, Utikal J. The Role of Myeloid-Derived Suppressor Cells (MDSC) in Cancer Progression. Vaccines (Basel). 2016; 4:36.
https://doi.org/10.3390/vaccines4040036
PMID:27827871

47. Zhou Y, Xiao L, Long G, Cao J, Liu S, Tao Y, Zhou L, Tang J. Identification of senescence-related subtypes, establishment of a prognosis model, and characterization of a tumor microenvironment

infiltration in breast cancer. Front Immunol. 2022; 13:921182.
https://doi.org/10.3389/fimmu.2022.921182
PMID:36072578

48. Botta C, Gullà A, Correale P, Tagliaferri P, Tassone P. Myeloid-derived suppressor cells in multiple myeloma: pre-clinical research and translational opportunities. Front Oncol. 2014; 4:348.
https://doi.org/10.3389/fonc.2014.00348
PMID:25538892

49. Bryant C, Suen H, Brown R, Yang S, Favaloro J, Aklilu E, Gibson J, Ho PJ, Iland H, Fromm P, Woodland N, Nassif N, Hart D, Joshua DE. Long-term survival in multiple myeloma is associated with a distinct immunological profile, which includes proliferative cytotoxic T-cell clones and a favourable Treg/Th17 balance. Blood Cancer J. 2013; 3:e148.
https://doi.org/10.1038/bcj.2013.34
PMID:24036947

50. Büttner R, Longshore JW, López-Ríos F, Merkelbach-Bruse S, Normanno N, Rouleau E, Penault-Llorca F. Implementing TMB measurement in clinical practice: considerations on assay requirements. ESMO Open. 2019; 4:e000442.
https://doi.org/10.1136/esmoopen-2018-000442
PMID:30792906

51. Petitprez F, Meylan M, de Reyniès A, Sautès-Fridman C, Fridman WH. The Tumor Microenvironment in the Response to Immune Checkpoint Blockade Therapies. Front Immunol. 2020; 11:784.
https://doi.org/10.3389/fimmu.2020.00784
PMID:32457745

52. Rowshanravan B, Halliday N, Sansom DM. CTLA-4: a moving target in immunotherapy. Blood. 2018; 131:58–67.
https://doi.org/10.1182/blood-2017-06-741033
PMID:29118008

53. Xu C, Xu H, Liu B. Head and neck squamous cell carcinoma-specific prognostic signature and drug sensitive subtypes based on programmed cell death-related genes. PeerJ. 2023; 11:e16364.
https://doi.org/10.7717/peerj.16364 PMID:38025757

54. Hong X, Yu C, Bi J, Liu Q, Wang Q. TIGIT may Serve as a Potential Target for the Immunotherapy of Renal Cell Carcinoma. Adv Biol (Weinh). 2024; 8:e2300050.
https://doi.org/10.1002/adbi.202300050
PMID:37690824

55. Kulikowska de Nałęcz A, Ciszak L, Usnarska-Zubkiewicz L, Frydecka I, Pawlak E, Szmyrka M, Kosmaczewska A. Deregulated Expression of Immune Checkpoints on Circulating CD4 T Cells May Complicate Clinical Outcome and Response to Treatment with Checkpoint

Inhibitors in Multiple Myeloma Patients. Int J Mol Sci. 2021; 22:9298.
https://doi.org/10.3390/ijms22179298
PMID:34502204

56. Sharma P, Yadav P, Sundaram S, Venkatraman G, Bera AK, Karunagaran D. HMGB3 inhibition by miR-142-3p/sh-RNA modulates autophagy and induces apoptosis via ROS accumulation and mitochondrial dysfunction and reduces the tumorigenic potential of human breast cancer cells. Life Sci. 2022; 304:120727.
https://doi.org/10.1016/j.lfs.2022.120727
PMID:35753437

57. Poorghobadi S, Hosseini SY, Sadat SM, Abdoli A, Irani S, Baesi K. The Combinatorial Effect of Ad-IL-24 and Ad-HSV-tk/GCV on Tumor Size, Autophagy, and UPR Mechanisms in Multiple Myeloma Mouse Model. Biochem Genet. 2025; 63:315–30.
https://doi.org/10.1007/s10528-024-10671-2
PMID:38436816

58. Bisht K, Fukao T, Chiron M, Richardson P, Atanackovic D, Chini E, Chng WJ, Van De Velde H, Malavasi F. Immunomodulatory properties of CD38 antibodies and their effect on anticancer efficacy in multiple myeloma. Cancer Med. 2023; 12:20332–52.
https://doi.org/10.1002/cam4.6619
PMID:37840445

59. Zhang MJ, Gao W, Liu S, Siu SP, Yin M, Ng JC, Chow VL, Chan JY, Wong TS. CD38 triggers inflammasome-mediated pyroptotic cell death in head and neck squamous cell carcinoma. Am J Cancer Res. 2020; 10:2895–908.
PMID:33042624

60. Bae J, Kitayama S, Herbert Z, Daheron L, Kurata K, Keskin DB, Livak K, Li S, Tarannum M, Romee R, Samur M, Munshi NC, Kaneko S, et al. Differentiation of BCMA-specific induced pluripotent stem cells into rejuvenated CD8αβ+ T cells targeting multiple myeloma. Blood. 2024; 143:895–911.
https://doi.org/10.1182/blood.2023020528
PMID:37890146

61. Li Z, Ma R, Tang H, Guo J, Shah Z, Zhang J, Liu N, Cao S, Marcucci G, Artis D, Caligiuri MA, Yu J. Therapeutic application of human type 2 innate lymphoid cells via induction of granzyme B-mediated tumor cell death. Cell. 2024; 187:624–41.e23.
https://doi.org/10.1016/j.cell.2023.12.015
PMID:38211590

62. Wu M, Li A, Zhang T, Ding W, Wei Y, Wan C, Ke B, Cheng H, Jin C, Kong C. The novel prognostic analysis of AML based on ferroptosis and cuproptosis related genes. J Trace Elem Med Biol. 2024; 86:127517.

https://doi.org/10.1016/j.jtemb.2024.127517
PMID:39270538

63. Liu K, Sun MM, Zhao ZH, Wei N, Jiang GZ, Wang ZY, Zhang L, Zhu XY, Dai LP, Yang HM, Wang T, Chen KS. Effect of RhoC silencing on multiple myeloma xenografts and angiogenesis in nude mice. J Biol Regul Homeost Agents. 2019; 33:1387–94.
PMID:31507136

64. Xu J, Liu B, Ma S, Zhang J, Ji Y, Xu L, Zhu M, Chen S, Wu X, Wu D. Characterizing the Tumor Suppressor Role of CEACAM1 in Multiple Myeloma. Cell Physiol Biochem. 2018; 45:1631–40.
https://doi.org/10.1159/000487730 PMID:29486474

65. Zhang M, Chen J, Zhang H, Dong H, Yue Y, Wang S. Interleukin-10 increases macrophage-mediated chemotherapy resistance via FABP5 signaling in multiple myeloma. Int Immunopharmacol. 2023; 124:110859.
https://doi.org/10.1016/j.intimp.2023.110859
PMID:37666065

66. Li H, Liu J, Wang S, Xu Y, Tang Q, Ying G. 4-Hydroxyphenylpyruate Dioxygenase-Like predicts the prognosis and the immunotherapy response of cancers: a pan-cancer analysis. Aging (Albany NY). 2024; 16:4327–47.
https://doi.org/10.18632/aging.205591
PMID:38451188

67. Zhou H, Xie T, Gao Y, Zhan X, Dong Y, Liu D, Xu Y. A novel prognostic model based on six methylation-driven genes predicts overall survival for patients with clear cell renal cell carcinoma. Front Genet. 2022; 86:127517.
https://doi.org/10.3389/fgene.2022.996291
PMID:36330441

68. Hu M, Xie J, Liu Z, Wang X, Liu M, Wang J. Comprehensive Analysis Identifying Wnt Ligands Gene Family for Biochemical Recurrence in Prostate Adenocarcinoma and Construction of a Nomogram. J Comput Biol. 2020; 27:1656–67.
https://doi.org/10.1089/cmb.2019.0397
PMID:32298604

69. Han T, Lin J, Wang Y, Fan Q, Sun H, Tao Y, Sun C. Forkhead box D1 promotes proliferation and suppresses apoptosis via regulating polo-like kinase 2 in colorectal cancer. Biomed Pharmacother. 2018; 103:1369–75.
https://doi.org/10.1016/j.biopha.2018.04.190
PMID:29864920

70. Li M, Qi L, Xu JB, Zhong LY, Chan S, Chen SN, Shao XR, Zheng LY, Dong ZX, Fang TL, Mai ZY, Li J, Zheng Y, Zhang XD. Methylation of the Promoter Region of the Tight Junction Protein-1 by DNMT1 Induces EMT-like Features in Multiple Myeloma. Mol Ther Oncolytics. 2020; 19:197–207.
https://doi.org/10.1016/j.omto.2020.10.004
PMID:33251332

71. Liu XQ, Shao XR, Liu Y, Dong ZX, Chan SH, Shi YY, Chen SN, Qi L, Zhong L, Yu Y, Lv T, Yang PF, Li LY, et al. Tight junction protein 1 promotes vasculature remodeling via regulating USP2/TWIST1 in bladder cancer. Oncogene. 2022; 41:502–14.
https://doi.org/10.1038/s41388-021-02112-w
PMID:34782718

72. Sabol HM, Delgado-Calle J. The multifunctional role of Notch signaling in multiple myeloma. J Cancer Metastasis Treat. 2021; 7:20.
https://doi.org/10.20517/2394-4722.2021.35
PMID:34778567

73. Delgado-Calle J, Anderson J, Cregor MD, Hiasa M, Chirgwin JM, Carlesso N, Yoneda T, Mohammad KS, Plotkin LI, Roodman GD, Bellido T. Bidirectional Notch Signaling and Osteocyte-Derived Factors in the Bone Marrow Microenvironment Promote Tumor Cell Proliferation and Bone Destruction in Multiple Myeloma. Cancer Res. 2016; 76:1089–100.
https://doi.org/10.1158/0008-5472.CAN-15-1703
PMID:26833121

74. Shirazi F, Jones RJ, Singh RK, Zou J, Kuiatse I, Berkova Z, Wang H, Lee HC, Hong S, Dick L, Chattopadhyay N, Orlowski RZ. Activating KRAS, NRAS, and BRAF mutants enhance proteasome capacity and reduce endoplasmic reticulum stress in multiple myeloma. Proc Natl Acad Sci USA. 2020; 117:20004–14.
https://doi.org/10.1073/pnas.2005052117
PMID:32747568

75. Guenther M, Boeck S, Heinemann V, Werner J, Engel J, Ormanns S. The impact of adjuvant therapy on outcome in UICC stage I pancreatic cancer. Int J Cancer. 2022; 151:914–9.
https://doi.org/10.1002/ijc.34044 PMID:35467760

76. Tao Y, Wei L, You H. Ferroptosis-related gene signature predicts the clinical outcome in pediatric acute myeloid leukemia patients and refines the 2017 ELN classification system. Front Mol Biosci. 2022; 9:954524.
https://doi.org/10.3389/fmolb.2022.954524
PMID:36032681

77. Zhu J, Zou H, Yu W, Huang Y, Liu B, Li T, Liang C, Tao H. Checkpoint kinase inhibitor AZD7762 enhance cisplatin-induced apoptosis in osteosarcoma cells. Cancer Cell Int. 2019; 19:195.
https://doi.org/10.1186/s12935-019-0896-9
PMID:31372095
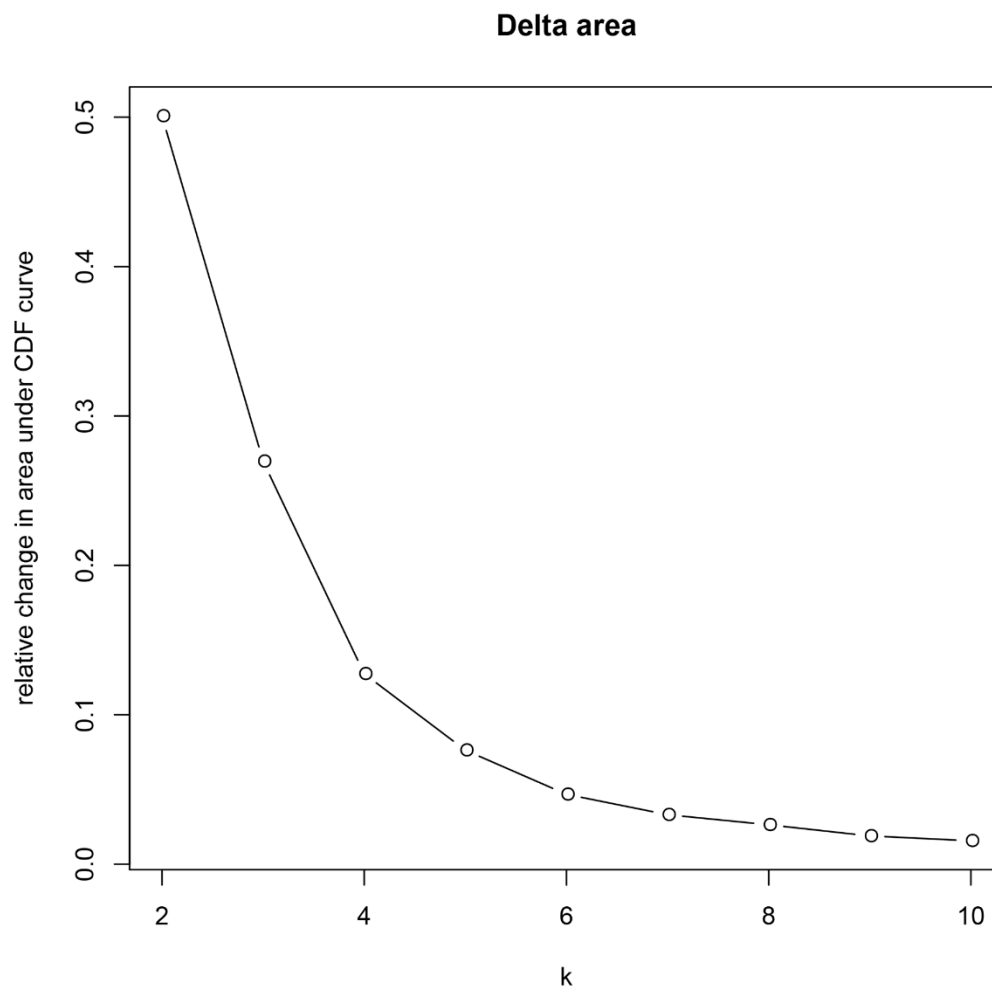
Supplementary Figure 1. Formulaic cluster analysis of MM prognosis-associated PCD genes. (S1) Horizontal coordinates indicate the number of categories k and vertical coordinates indicate the relative change in area under the CDF curve.